 DOI:10.30420/566414040

3.3kV SBD-Embedded SiC-MOSFET module for railway applications

Daichi Yosho[1], Yoichi Hironaka[1], Shigeru Okimoto[1], Jian Sun[2], Kenji Hatori[1]

[1] Mitsubishi Electric Corporation, 1-1-1 Imajukuhigashi, Nishi-Ku, Fukuoka, Japan
[2] Mitsubishi Electric & Electronics (Shanghai) Co., Ltd., China

Corresponding author: Daichi Yosho, Yosho.Daichi@dw.MitsubishiElectric.co.jp
Speaker: Daichi Yosho, Yosho.Daichi@dw.MitsubishiElectric.co.jp

Abstract

We have developed a new 3.3kV Schottky-barrier-diode-embedded (SBD-Embedded) silicon-carbide metal-oxide-semiconductor field-effect transistor (SiC-MOSFET) module that fulfills the high-reliability, high-power, and high-efficiency requirements of railway applications. It avoids the bipolar degradation inherent to SiC-MOSFET by embedding the SBD into the MOSFET. It also achieves sufficient surge current capability through the introduction of a novel structure, the bipolar mode activation (BMA) cell. When compared to the conventional SiC module, the electrical characteristics show a significant improvement, with a 58% reduction in switching losses. Furthermore, the thermal resistance is reduced by 35% in the MOSFET part and 63% in the free-wheeling diode part. Consequently, the output current for inverters is markedly enhanced.

1 Introduction

Since the latter half of the 1990s, silicon-based insulated gate bipolar transistors (IGBT) power semiconductors have been used for the railway applications. The performance of these applications has progressively improved through various improvements such as reducing losses and advancing packaging technologies. However, silicon-based power semiconductors are now nearing their physical limits, and in order to achieve more drastic improvements, it is essential to employ wide bandgap semiconductors like SiC. SiC power devices have been adopted relatively early in railway applications, and as of 2024, they have approximately a decade of field performance [1] [2].

A crucial role of SiC-MOSFET is ensuring reliability. The reliability needs to be equivalent to, or even greater than traditional Si-IGBT modules, but this presents a higher level of difficulty compared to Si-IGBT. This is because there are reliability issues unique to SiC-MOSFET that do not exist in Si-IGBT. One of these SiC-specific reliability issues is the increase in on-voltage due to bipolar degradation (see Fig. 1). How to prevent this bipolar degradation is the key to realizing high-reliability SiC-MOSFETs [3-5].

Equally important as reliability is the improvement of electrical characteristics, especially the reduction of energy loss. The reduction of switching and conduction losses in power devices directly leads to an increase in the efficiency of the application systems, which is extremely important. In addition, improving thermal characteristics is crucial because the SiC modules are expected to be used at high temperature. The enhancement of loss and thermal characteristics also contributes to an improvement in the module's lifespan. In other words, the low loss and thermal resistance characteristics of SiC-MOSFET module significantly contribute to the realization of high-efficiency and long-life railway application systems.

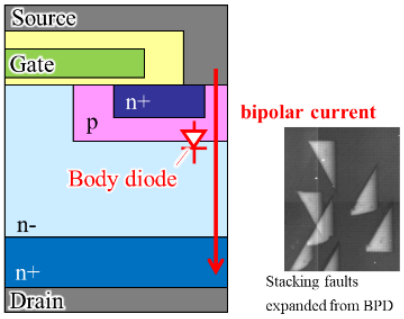

Fig. 1 Bipolar degradation of the body diode of SiC-MOSFETs.

ISBN 978-3-8007-6414-3

In this paper, we propose a 3.3kV SBD-Embedded SiC-MOSFET module characterized by high reliability, low loss, and low thermal resistance, along with the technical concept of the module. The applications of SiC-MOSFET module extend beyond main inverter units to auxiliary power units (APU), battery chargers, and DC-DC converters. As the suitable current capacity varies for each application, a comprehensive range of options is required to meet the demand accordingly. Consequently, we have expanded our new module lineup to accommodate various applications. As part of this lineup, we primarily report on the low current rating module suitable for applications such as APU.

2 Overview -3.3kV SBD-Embedded SiC-MOSFET module

The appearance of the newly developed module is shown in Fig. 2. For low package inductance and fast switching, the LV 100 package is used, which is the new standard for high-voltage power modules. This package is identical to the conventional 3.3kV full-SiC power module. Table 1 shows the lineup of 3.3 kV SBD-Embedded SiC-MOSFET module. We have a wide range of lineup including products with ratings of 800A, 400A, and 200A.

In the following sections, we delve into the details of the reliability, electrical characteristics, and thermal characteristics of these newly developed products. The electrical and thermal characteristics are explained using a low current rated product. Lastly, we describe the application advantages of these new developments.

Fig. 2 3.3kV SBD-Embedded SiC-MOSFET module.

Table 1. Lineup of 3.3kV SBD-Embedded SiC-MOSFET modules

Type name	Rated voltage	Rated current	Isolation voltage	Maximum junction temperature
FMF800DC-66BEW	3.3 kV	800 A	6.0 kV_{rms}	175 °C
FMF400DC-66BEW	3.3 kV	400 A	6.0 kV_{rms}	175 °C
FMF200DC-66BE	3.3 kV	200 A	6.0 kV_{rms}	175 °C

3 Reliability

3.1 Eliminate bipolar degradation

To realize a highly reliable SiC-MOSFET power module, it is necessary to overcome a unique issue for SiC-MOSFET, namely bipolar degradation caused by inherent diode conduction (cf. Fig. 1). One method to prevent bipolar degradation is to mount an SBD chip as a free-wheeling diode and to conduct special screening tests. However, the risk of bipolar degradation becomes significantly higher in high-voltage and high-power applications where the total chip area is large and the drift layer is thick. In conventional 3.3kV SiC-MOSFET modules, the SBD chip needs to be about 1.5 times the size of the MOSFET chip to keep the inherent diode inactive [3]. This requires valuable space within the power module and adds to the cost of manufacturing the power module. If the SBD is embedded into the MOSFET chip, the required chip area can be reduced and the special screening tests are unnecessary.

The difference between the external SBD and embedded SBD is explained bellow. The voltage drop through the external SBD needs to be lower than the built-in potential of the PN junction of the paralleled MOSFET to prevent the inherent diode operation. As the required breakdown voltage increases, the drift layer of the external SBD becomes thicker, and the voltage drop becomes larger. Fig. 3 illustrates the schematic circuit of a conventional SiC-MOSFET coupled with an external SBD and SBD-Embedded SiC-MOSFET. In the case of an external SBD, the total voltage drop across the chip is applied to the PN junction of the MOSFET. In contrast, in the SBD-Embedded MOSFET, the drift layer is shared, so the voltage drop in the drift layer is not applied to the PN junction. Therefore, it is possible to suppress the conduction of the inherent diode without a significant increase in the required chip area. Fig. 4 demonstrates the processes of inactivating the inherent body diode by incorporating the SBD into the chip. (a) shows a structure where the MOSFET and SBD sections are largely divided, equivalent to the case with an external SBD chip. In this case, when the voltage drop of SBD part and drift-layer exceed the built-in potential of the inherent diode, the inherent body diode begins to conduct. Here, the current density at which the inherent body diode begins to conduct is defined as the maximum unipolar current density (J_{SD}). In (b), the repetition pitch of the MOSFET and SBD is shortened, which increases the maximum unipolar current density. In (c), by reducing the pitch to the unit cell size, it is possible to suppress the inherent diode up to a large current density. In the case of (c), the J_{SD} is increased to the level where the SBD operates and the inherent body diode does not operate within the normal operating range.

 DOI:10.30420/566414040

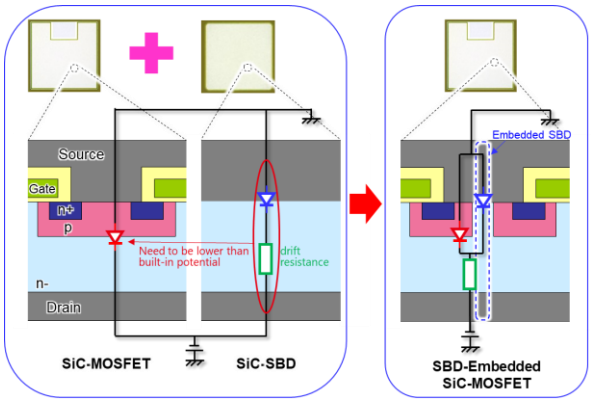

Fig. 3 Schematic circuit of a conventional SiC-MOSFET coupled with an external SBD and SBD-Embedded SiC-MOSFET

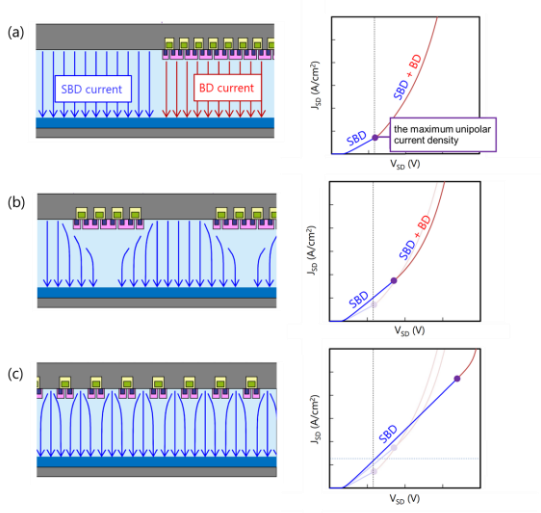

Fig. 4 Processes of inactivating the inherent body diode by incorporating the SBD into the chip

3.2 Enhance surge current capability

It has been noted that SBD-Embedded SiC-MOSFETs have the disadvantage of lower surge current capability compared to the bipolar devices that utilize body diodes because embedded SBDs hinder conductivity modulation during a surge and resulting in high conduction losses in the high-current region. While the fact that SBD-Embedded SiC-MOSFETs do not undergo bipolar conduction is advantageous in terms of preventing degradation, it also results in a reduced surge current capability. To address these seemingly contradictory issues, we propose the novel structure for improving the surge current capability of SBD-Embedded SiC-MOSFETs. Fig. 5 shows the novel structure. Some part of the built-in SBD is filled with p-body to inactivate the corresponding SBDs and we refer to this novel structure as a bipolar mode activation cell (BMA cell) [6] [7]. With BMA cells implemented, the surge current capability of the SBD-Embedded SiC-MOSFET module reaches a similar level to that of the body-diode-operated SiC-MOSFET module (See Fig. 6, showing the results of the 800A product.) [8]. For reference, Fig. 6 also shows the measurement results of a 600 A Si module with Si-diode chips of similar module rating specifications, at an initial junction temperature of T_j = 125 °C. The SBD-Embedded SiC-MOSFET module also demonstrates better surge current capability than that of conventional Si module even at 50 K higher initial temperature. Below, we provide details about the BMA cells.

The BMA cell fulfills two primary functions. First, it triggers the operation of the inherent body diodes only under circumstances that necessitate surge current capability, that is, when a substantial accident current flows under abnormal conditions. The conduction of the body diodes contributes to the enhancement of the surge current capability by suppressing conduction losses during high current flow. The impact of bipolar degradation due to the current conduction of the inherent body diodes can be disregarded. This is because it only occurs in limited situations such as emergencies, thereby minimizing the risk of such degradation as much as possible. The area of the BMA cell is about 0.2% of the total chip area, and it does not affect the electrical characteristics. Naturally, the body diodes remain inactive during regular operation. Fig. 7 illustrates the I-V characteristics at T_j = 175 °C of SBD-Embedded SiC-MOSFETs, both with and without BMA cells, signifying unipolar operation within the safe operating area of the power module in both scenarios.

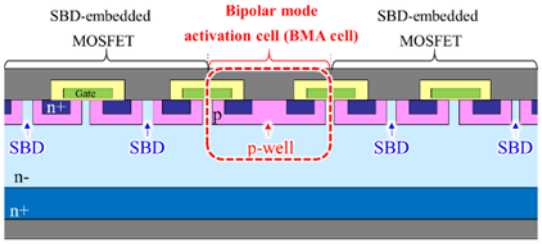

Fig. 5 Structure of BMA cell

 DOI:10.30420/566414040

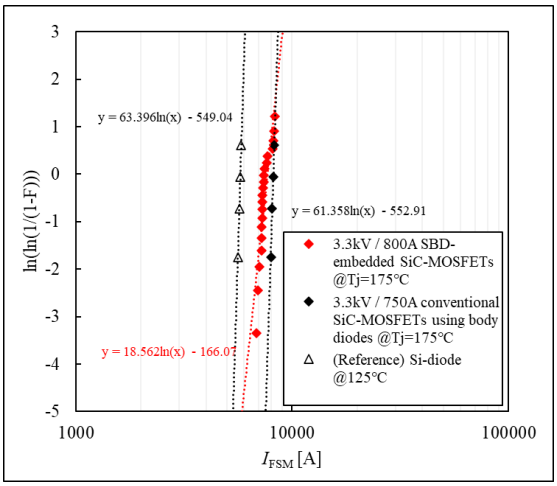

Fig. 6 Weibull plots of surge forward current (I_{FSM}) measurement results.

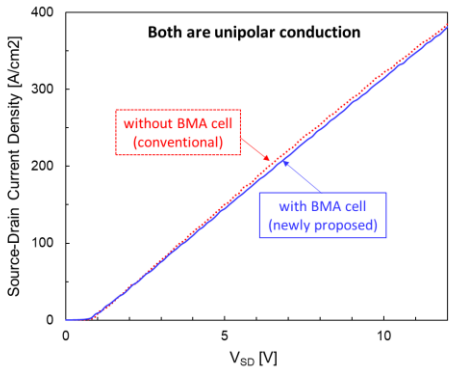

Fig. 7 Source-drain current density and source-drain voltage (V_{SD}) waveforms at T_j=175 °C of SBD-Embedded SiC-MOSFETs.

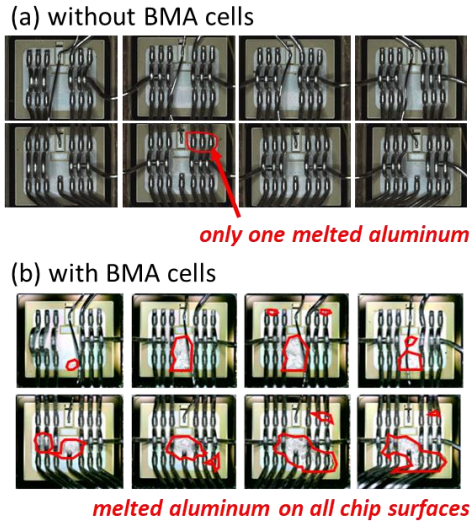

Fig. 8 Surface appearance of chips conected in parallel after test of surge current capability.

Second, the BMA cell mitigates the characteristic variation of each SBD-Embedded SiC-MOSFET chip installed in the module, particularly the snapback voltage. The voltage at which the inherent body diodes operate is defined as the snapback voltage (V_{snap}). In large-current power modules, multiple chips are typically mounted and interconnected in parallel, and the surge current capability of the power module does not equate to the sum of the surge current capability (I_{FSM} or I^2t) of the individual chips. This is because the current flow is concentrated on the chip with the smallest snapback voltage, where the transition from unipolar to bipolar behavior occurs ahead of all other chips. This hypothesis is substantiated by Fig. 8 (a), which depicts the appearance of the chips without BMA cells connected in parallel after the evaluation of the surge current capability. The presence of a melted aluminum area on the chip surface indicates that a large current has passed through the chip. It has been confirmed that the melting area is observed only on one chip. This suggests that the current is concentrated only on one chip where the melted aluminum is visible. The variation of the snapback voltage is significantly influenced by the width of the built-in SBD area within the SiC-MOSFET chip. Due to manufacturing variations, the width of the built-in SBD is challenging to control entirely. Therefore, by intentionally incorporating the body diode region, the variation of the snapback voltage can be minimized, and the snapback voltage can be controlled. With BMA cells (see Fig. 8 (b)), melted aluminum is visible and on the entire chip surface, indicating that the surge current is evenly distributed.

While Fig. 8 (b) shows the surge current evenly distribute across all chips, appropriate design of the BMA cell area is necessary to consistently create this state. This is because there is a correlation between the area of the BMA cell and the snapback voltage, with the snapback voltage decreasing as the BMA cell area is increased. To control the snapback voltage (and thus the surge current capability) by design, it is necessary to determine the BMA cell area to allow bipolar conduction at a voltage lower than the minimum snapback voltage, which varies due to the width variation of the embedded SBD in manufacturing. Fig. 9 shows the surge current capability and the number of chips where current is concentrated when the BMA cell area is changed. Two types of samples, α and β is prepared and the number of parallel chips in sample is four. Sample types of α and β have different BMA cell areas, with β's BMA cell area being 2.5 times larger than that of α. With α, the surge current capability is low as the current is concentrated in some chips. Even among the α samples, it is found that the more chips have melted aluminum on their surface, in other words, the more chips have concentrated current, the greater the surge current capability tends to be.

ISBN 978-3-8007-6414-3

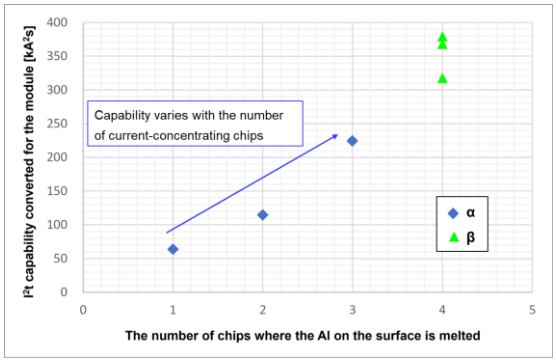

Fig. 9 The surge current capability and the number of chips where current is concentrated. BMA cell area of β is 2.5 times larger than that of α.

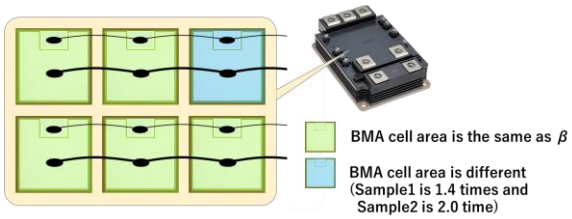

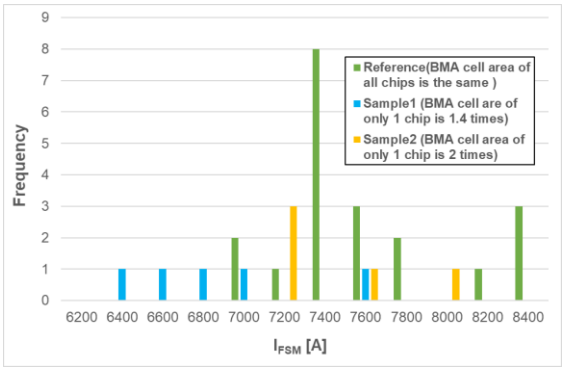

Fig. 10 Schematic diagram of sample specifications and results of surge current capability.

On the other hand, with β, the current flows evenly across all chips, resulting in high surge current capability. Therefore, there are no issues with surge current capability when designing with the BMA cell area of 'β' or more. Although the number of samples in Fig. 9 is three for each specification, we have conducted a sufficient number of evaluations for modules assembled with chips of BMA cell area with equivalent or greater β. In that module evaluation, we have confirmed that the current is evenly distributed and the module has sufficient surge current capability (cf. Fig. 6).

Taking into account the manufacturing variation of the BMA cell itself, it is also necessary to confirm whether the current is evenly distributed to all parallel chips (i.e., it has a high surge current capability) even if the BMA cell area is scattered. Two types of experimental samples, sample1 and sample2, were prepared and the BMA cell area of only one of the parallel chips in the module was different. The exceptional chip in sample1 is 1.4 times and in sample2 is 2 times larger than that of all other chips in the module. Excluding that exceptional one chip, all chips in module have a BMA cell area that is unified to be equivalent to β (see the upper part of Fig. 10). The number of samples is five for each type and the surge current capability of those samples was measured. The results in the lower part of Fig. 10 shows that even if the BMA cell area is scattered up to 2 times, it does not significantly affect the surge current capability. Following the evaluation test, the module was disassembled and the melting marks of the aluminum on the chip surface were examined. The appearance was similar to that of Fig. 8 (b), and it was found that the current was not concentrated on only one chip where the BMA cell area was intentionally altered but was instead distributed. In other words, it means that a module with parallel-connected SBD-Embedded MOSFET chips with built-in BMA cells has a stable surge current capability, unaffected by manufacturing variations of BMA cell.

4 Electrical characteristics

The newly developed SBD-Embedded SiC-MOSFET module dramatically improves switching characteristics compared to the conventional full-SiC module. Fig. 11 shows a comparison of the switching waveforms of the newly developed module (FMF400DC-66BEW) and the conventional module (FMF375DC-66A). To make a fair comparison, the switching conditions are aligned with each other, with drain-source voltage V_{DS}=1800V, drain current I_D=375A, stray inductance in commutation circuit L_S=40nH, gate resistance $R_{G(ON)}$=1.5Ω, $R_{G(OFF)}$=3.0Ω, operating temperature T_j=175°C. From the switching waveforms, the following two features can be observed.

Firstly, the turn-on and turn-off switching delay time of the newly developed module is decreased (i.e., higher switching speed) compared to the conventional module. The enhancements of switching speed are realized through an optimized chip design, which leads to a decrease in input capacitance (C_{iss}) and an increase in mutual conductance (g_m). We optimized the channel layout, improved the mutual conductance, and increased the dI_D/dt. C_{iss} is measured under the following conditions: drain-source voltage V_{DS} = 10 V, gate-source voltage V_{GS} = 0 V, frequency f = 100 kHz. As depicted in Fig. 12, g_m is evaluated by determining dI_D/dV_{GS} near the rated current. The measurements of C_{iss} and g_m are provided in Table 2, indicating a 48% decrease in Ciss and a 41 % increase in g_m when comparing the new FMF400DC-66BEW with the conventional FMF375DC-66A. As a result, the newly developed module demonstrates diminished turn-on and turn-off switching delay times, contributing to a reduction in switching losses.

Fig. 11(a) Turn-on and turn-off of diode switching waveforms (V_{DD}=1800V, I_D=I_S=375A, $R_{G(ON)}$=1.5Ω, $R_{G(OFF)}$=3.0Ω, L_S=40nH, T_j=175 °C)

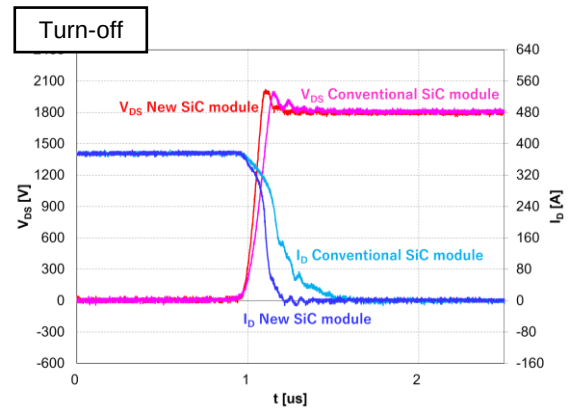

Fig. 11(b) Turn-off switching waveform. (V_{DD}=1800V, I_D=375A, L_S=40nH, $R_{G(ON)}$=1.5Ω, $R_{G(OFF)}$=3.0Ω T_j=175 °C)

Table 2. Comparison of capacitance and conductance characteristics.

	C_{iss}	g_m
Conventional module (FMF375DC-66A)	105 nF	134 Ω^{-1}
Newly developed module (FMF400DC-66BEW)	55 nF	189 Ω^{-1}

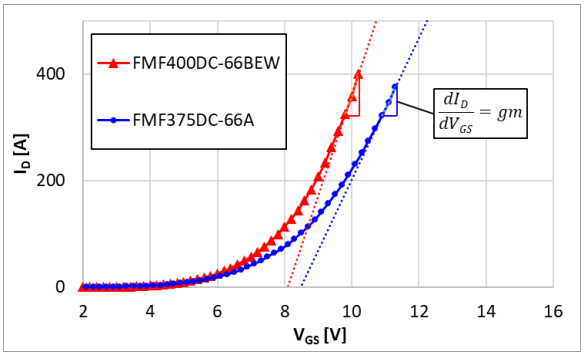

Fig. 12 Drain current (I_D) and gate-source voltage (V_{GS}) characteristics.
(Drain-source voltage (V_{DS}) = 20V, T_j = 25 °C).

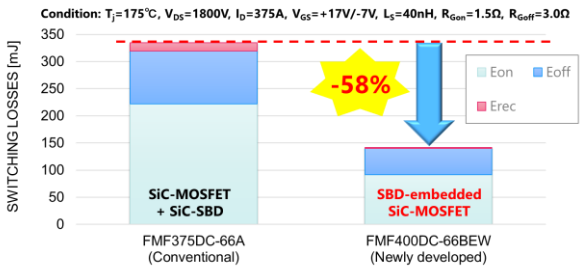

Fig. 13 Comparison of the switching losses. (V_{DD}=1800V, I_D=375A, L_S=40nH, $R_{G(ON)}$=1.5Ω, $R_{G(OFF)}$=3.0Ω, T_j=175 °C)

Secondly, the SBD-Embedded SiC-MOSFET module has fewer emitted carriers during the turn-off switching of diode (the recovery, as referred to in PN diodes). The reason is that it utilizes an embedded SBD and there is no recovery current (only displacement current for charging and discharging the output capacitance). If an inherent body diode was used, the quantity of emitted carriers during the turn-off switching of diode would be higher, that is, the recovery current flows. In the conventional module, an external SBD was connected, but it did not completely suppress recovery charge by minority carrier injection. This results in a small amount of reverse recovery current (see the lower part of Fig. 11 (a)). This is the reason why the new module has lower losses of the turn-off switching of diode. Additionally, since the current during the turn-off switching of diode (recovery current) influences the increase in turn-on current of the opposing switching arm. In other words, the SBD-Embedded SiC-MOSFET also achieves a reduction in turn-on switching losses since it does not have a current for the turn-off switching of diode.

Fig. 13 shows a comparison of the switching losses of the SBD-Embedded SiC-MOSFET (FMF400DC-66BEW) and the conventional full-SiC module (FMF375DC-66A). The switching conditions are equivalent to those in Fig. 11. The SBD-Embedded SiC-MOSFET module has achieved a 58% reduction in the total switching losses.

 DOI:10.30420/566414040

5 Thermal characteristics

The thermal characteristics are crucial for SiC modules as they are designed for operation at high temperature. Fig. 14 illustrates the cross-section of the module. To operate at high temperature (maximum junction temperature T_{jmax} = 175 °C), the chips are bonded using silver (Ag) sintering, and the terminals are connected to the substrate by ultra-sonic bonding. The newly developed modules exhibit low thermal resistance (R_{th}) because thermally improved materials of substrate and solder are adopted. Moreover, the low current rating modules (400A rating and 200A rating) have a reduced number of chips compared to the 800A rating module, allowing for flexibility in chip layout. Consequently, by optimizing the chip placement, it is possible to further decrease the thermal resistance. To determine a chip layout that results in lower thermal resistance, we conducted simulations of thermal interference between chips. Fig. 15 shows a schematic of thermal interference and an example of the results from the thermal simulation. The thermal resistance varies by changing the distance between multiple chips. If the chips are too close together, the thermal interference increases, leading to a higher thermal resistance. Conversely, if they are too far apart, the chips approach the edge of the module, limiting heat dissipation and consequently increasing thermal resistance. Therefore, it is necessary to design with an optimal chip spacing. Furthermore, we have confirmed that the measurement result of thermal resistance for the module with the optimal chip distance and the simulation result (as shown in Fig.15) are almost identical. Fig. 16 compares the thermal resistance values between the conventional and newly developed module, indicating a reduction of 35% in the MOSFET part and 63% in the free-wheeling diode part.

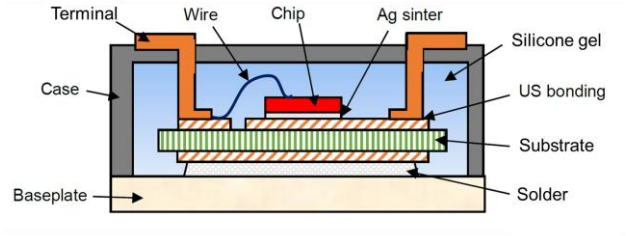

Fig. 14 Cross-sections of SBD-Embedded SiC-MOSFET module.

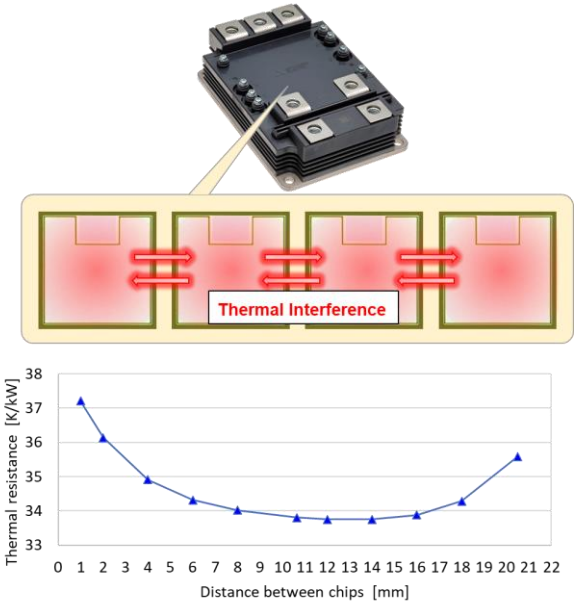

Fig. 15 Schematic diagram of thermal interference between chips, and an example of simulation results of thermal interference when changing the distance between multiple chips

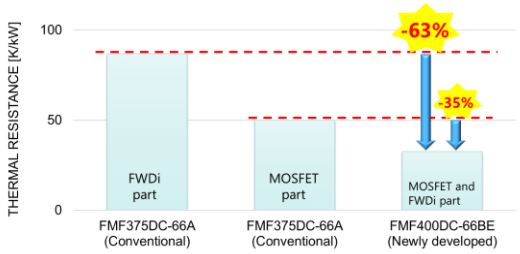

Fig. 16 Comparison of the thermal resistances .

6 Application benefit -Inverter output current simulation

Improvements in the power module performance is directly linked to the efficiency of application. Here, we calculate the frequency dependence of the output current of the inverter using the Melcosim power loss simulator [9]. Inverter output current is commonly used as a benchmark for assessing overall device performance. Fig. 17 shows the frequency dependence of the output current of the inverter. The blue line is newly developed SBD-Embedded SiC-MOSFET module, FMF400DC-66BEW and the red line is conventional full-SiC module, FMF375DC-66A. The simulation was conducted under the following conditions: supply voltage V_{DD} = 1800 V, power factor P.F. = 0.85, heat sink temperature T_S = 80 °C, modulation ratio = 1. The gate-drive conditions applied the recommended conditions for each power module.

ISBN 978-3-8007-6414-3

The output current from the inverter of the newly developed module is observed to surpass that of the conventional full-SiC module across the entire frequency spectrum. Significantly, at a frequency of 3 kHz, the output current from the inverter of the new module is more than 40% higher than that of the conventional full-SiC module. This information confirms that the new module delivers exceptional inverter output. That is to say, the newly developed module contributes to the dramatic efficiency improvements not only in the main traction systems, but also in applications such as the APU, which are generally used in the high-frequency range.

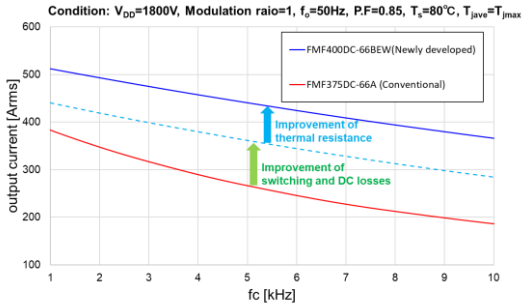

Fig. 17 Simulation results of inverter output current. V_{DD} = 1800 V, P.F. = 0.85, T_S = 80 °C, modulation ratio = 1.

7 Conclusion

The application of SiC-MOSFET power modules with higher efficiency than that of Si-IGBTs is advancing in the railway field. Essential to SiC-MOSFET modules are superior characteristics that contribute to high-reliability, low-energy-loss, and low-thermal-resistance. Considering these elements, we have developed an SBD-Embedded SiC-MOSFET module as a next-generation SiC module and prepared a lineup with a wide current rating. By incorporating SBD into MOSFET, bipolar degradation is prevented, ensuring high reliability. By introducing a new structure called the BMA cell, we have overcome the problem of surge current capability, which was said to be a weakness of the SBD-Embedded SiC-MOSFET, and additionally confirmed that it is a technology that can cope with manufacturing variations. The improvement of electrical characteristics has reduced the switching loss by 58% compared to the conventional module. In addition, improvements in structural components and optimization of thermal design have significantly reduced the thermal resistance especially of low-current products compared to the conventional module. The improvements in electrical characteristics and thermal resistance have also significantly improved the output current of the inverter, with particularly great benefits in the high-frequency range.

8 References

[1] S. Hatsukade, "A Survey of the Adoption of SiC Semiconductor for Power Devices in Railway Vehicles in Japan and Overseas," Railway Technical Research Institute Report, vol. 36, no. 2, pp. 35-40, 2022.

[2] Mitsubishi Electric Press Release No. 2942, Mitsubishi Electric Installs Railcar Traction System with All-SiC Power Modules on Shinkasen Bullet Train, Japan, 2015.

[3] T. Tominaga, S. Hino, Y. Mitsui, J. Nakashima, K. Kawahara, S. Tomohisa, N. Miura, “Inves-tigation on the Effect of Total Loss Reduction of HV Power Module by Using SiC-MOSFET Embedding SBD”, Materials Science Forum 2020, vol. 1004, pp. 801-807

[4] M. Furukawa, H. Kono, K. Sano, M. Yamagu-chi, H. Suzuki, T. Misao, G. Tchouangue, “Improved reliability of 1.2kV SiC MOSFET by preventing the intrinsic body diode operation”, PCIM Europe digital days 2020, pp. 1- 5

[5] T. Ishigaki, T. Murata, K. Kinoshita, T. Mori-kawa, T. Oda, R. Fujita, K. Konishi, Y. Mori, A. Shima, “Analysis of Degradation Phenomena in Bipolar Degradation Screening Process for SiC-MOSFETs”, Proceedings of ISPSD’19, pp. 259-262

[6] A. Iijima, K. Kawahara, K. Sugawara, S. Hino, K. Fujiyoshi, Y. Oritsuki, T. Murakami, T. Takahashi, Y. Kagawa, Y. Hironaka, K. Nishi-kawa, “Improving Surge Current Capability of SBD-Embedded SiC-MOSFETs in Parallel Connection by Applying Bipolar Mode Activa-tion Cells”, Proceedings of ISPSD’23, pp. 238-241

[7] K. Kawahara, K. Sugawara, A. Iijima, K. Fuji-yoshi, Y. Oritsuki, T. Murakami, T. Takahashi, Y. Kagawa, Y. Hironaka, K. Nishikawa, “Comparison of the Surge Current Capabilities of SBD-Embedded and Conventional SiC MOSFETs”, Proceedings of ICSCRM 2023

[8] S. Okimoto, Y. Hironaka, K. Hatori, A. Iijima, K. Kawahara, K. Sugawara, N. Soltau, “Im-provement of Surge Current Capability of 3.3 kV SBD-Embedded SiC-MOSFET Module”, Proceedings of EPE’23 ECCE Europe, No. 042

[9] Melcosim download page: https://www.mitsubishielectric.com/semiconductors/simulator/index.html

